© 2014. Published by The Company of Biologists Ltd | Journal of Cell Science (2014) 127, 2518–2527 doi:10.1242/jcs.144220

RESEARCH ARTICLE

The scaffold protein MUPP1 regulates odorant-mediated signaling in olfactory sensory neurons

Sabrina Baumgart[1], Fabian Jansen[1], Willem Bintig[2], Benjamin Kalbe[1], Christian Herrmann[3], Fabian Klumpers[3], S. David Köster[4], Paul Scholz[1], Sebastian Rasche[1], Ruth Dooley[5], Nils Metzler-Nolte[6], Marc Spehr[7], Hanns Hatt[1] and Eva M. Neuhaus[2,8,*]

ABSTRACT

The olfactory signal transduction cascade transforms odor information into electrical signals by a cAMP-based amplification mechanism. The mechanisms underlying the very precise temporal and spatial organization of the relevant signaling components remains poorly understood. Here, we identify, using co-immunoprecipitation experiments, a macromolecular assembly of signal transduction components in mouse olfactory neurons, organized through MUPP1. Disruption of the PDZ signaling complex, through use of an inhibitory peptide, strongly impaired odor responses and changed the activation kinetics of olfactory sensory neurons. In addition, our experiments demonstrate that termination of the response is dependent on PDZ-based scaffolding. These findings provide new insights into the functional organization, and regulation, of olfactory signal transduction.

KEY WORDS: MUPP1, PDZ, Olfactory neuron, Scaffolding protein

INTRODUCTION

The function of the olfactory signal transduction cascade in the cilia of olfactory sensory neurons is to convert olfactory receptor activation into action potentials. Upon odorant binding, the receptors activate adenylyl cyclase type-III (ACIII, also known as ADCY3) (Bakalyar and Reed, 1990) through $G\alpha_{olf}$. The resulting rise in cAMP opens a nonselective cyclic-nucleotide-gated (CNG) cation channel, leading to an influx of Ca^{2+} and Na^{+} (Dhallan et al., 1990). As Ca^{2+} concentrations increase, Cl^{-} channels of the anoctamin family are activated in the ciliary membrane (Billig et al., 2011; Rasche et al., 2010; Stephan et al., 2009), leading to further depolarization. The Cl^{-} currents are maintained by the $Na^{+}/K^{+}/Cl^{-}$ co-transporter NKCC1, the Cl^{-}/HCO_3^{-} exchanger SLC4A1, and possibly additional, as yet unknown, transporters (Hengl et al., 2010; Nickell et al., 2007; Reisert et al., 2005). Response termination directly depends on cAMP degradation through phosphodiesterases and Ca^{2+} extrusion (Cygnar and Zhao, 2009). Simultaneously, the Ca^{2+} influx triggers, through Ca^{2+}-calmodulin, multiple negative-feedback pathways that lead to adaptation (Kleene, 2008; Zufall and Leinders-Zufall, 2000) and regulates the dynamic range of a given olfactory sensory neuron by mobilization of mitochondrial Ca^{2+} concentrations (Fluegge et al., 2012).

In the case of unitary responses that are triggered by individual odorant-binding events, spatially and functionally segregated ciliary transduction domains have been described (Bhandawat et al., 2005; Bhandawat et al., 2010). Additionally, recordings of Ca^{2+} changes in individual cilia using fluorescent Ca^{2+} indicator dyes have shown that Ca^{2+} microdomains exist, which contain one to three CNG channels (Castillo et al., 2010). Evidence exists for a role of lipid membrane microdomains in the organization of olfactory signaling proteins (Bockaert et al., 2004; Kobayakawa et al., 2002; Schreiber et al., 2000), but the impact of protein–protein interactions as the physical basis for the formation of chemosensory transduction microdomains, and the organization of discrete molecular signaling complexes, has not been characterized to date.

Post synaptic density 95, *Drosophila* discs large, zona occludens 1 (PDZ)-domain-containing scaffolding proteins regulate the assembly of different membrane-associated proteins and signaling molecules into a diverse range of macromolecular complexes. A well-known example is the inactivation no afterpotential D (InaD) protein in the visual system of *Drosophila melanogaster*, which is essential for high sensitivity, fast response activation and termination of light-induced currents through binding to rhodopsin and multiple other signaling-cascade members (Scott and Zuker, 1998; Xu et al., 1998). We have recently identified a putative organizer of olfactory signaling by showing that olfactory receptors interact with the multi-PDZ-domain protein MUPP1 (also known as MPDZ) (Dooley et al., 2009). MUPP1 comprises an L27 domain and 13 PDZ domains (Ullmer et al., 1998), rendering it an ideal candidate for the assembly of a multiprotein scaffold at olfactory-receptor-containing membrane sites. In the present study, we provide the first evidence that scaffolding processes involving PDZ-domain proteins play a crucial role in the organization of olfactory signal transduction by showing that MUPP1 forms a protein complex between key olfactory transduction components and regulates different aspects of signaling in olfactory neurons.

RESULTS

MUPP1 interacts with olfactory signaling proteins

We have previously shown that MUPP1 is expressed in the olfactory epithelium and that it can interact with olfactory receptors that have been expressed recombinantly (Dooley et al.,

[1]Cell Physiology, Faculty for Biology and Biotechnology, Ruhr-Universität Bochum, Universitätsstrasse 150, 44780 Bochum, Germany. [2]Cluster of Excellence NeuroCure, Charité-Universitätsmedizin Berlin, Charitéplatz 1, 10117 Berlin, Germany. [3]Physical Chemistry I, Ruhr-Universität Bochum, Universitätsstrasse 150, 44780 Bochum, Germany. [4]Inorganic Chemistry I - Bioinorganic Chemistry, Ruhr-Universität Bochum, Universitätsstrasse 150, 44780 Bochum, Germany. [5]Department of Molecular Medicine, Royal College of Surgeons in Ireland, Beaumont Hospital, Dublin 9, Ireland. [6]Chair of Inorganic Chemistry I - Bioinorganic Chemistry, Ruhr-Universität Bochum, Universitätsstrasse 150, 44780 Bochum, Germany. [7]Department of Chemosensation, Institute for Biology II, RWTH-Aachen University, Worringer Weg 1, 52074 Aachen, Germany. [8]Pharmacology and Toxicology, University Hospital Jena, Drakendorfer Weg 1, 07743 Jena, Germany.

*Author for correspondence (eva.neuhaus@med.uni-jena.de)

Received 10 October 2013; Accepted 9 March 2014

Journal of Cell Science (2014) 127, 2518–2527 doi:10.1242/jcs.144220

2009). As MUPP1 has multiple protein–protein interaction sites, we aimed to identify interaction partners of MUPP1 in sensory neurons by using co-immunoprecipitation analysis. To investigate the interaction with endogenously expressed olfactory receptors, we generated an antibody against the olfactory receptor protein Olfr73 and showed specificity by immunohistochemical staining and western blot analysis of Olfr73-transfected HEK293 cells (Fig. 1A). On cryosections of olfactory epithelium (Fig. 1B), the antibody specifically labeled only the cilia emanating from Olfr73-expressing neurons, which can be identified by expression of enhanced green fluorescent protein (eGFP) (Oka et al., 2006).

Co-immunoprecipitations in lysates of adult murine olfactory epithelium demonstrated that MUPP1 forms complexes with CNGA4, ACIII, $G\alpha_{olf}$, calmodulin, Olfr73 and Tmem16b (also known as Ano2) (Fig. 1C,D), all of which are well-known proteins that are involved in olfactory signal transduction. We found no detectable interaction with CNGA2 (Fig. 1C,D), which is probably due to technical difficulties, because we also failed to detect CNGA2 after precipitation of CNGA4, a binding partner of CNGA2 (Zheng and Zagotta, 2004) (data not shown). IgG control experiments did not show any signals. To complement the interaction analysis with *in vitro* studies, we analyzed whether recombinantly expressed and purified G_{olf} and ACIII bind to a purified PDZ domain of MUPP1. We expressed G_{olf} and ACIII in HEK293 cells and purified the proteins by binding to specific antibodies that were coupled to dynabeads. After washing of the dynabead-bound protein, we incubated the beads with PDZ domain 13 of MUPP1, which had been expressed as a GST fusion protein in *Escherichia coli* and purified. This analysis revealed that both of the purified proteins G_{olf} and ACIII can form complexes with a PDZ domain of MUPP1 (Fig. 1E).

Because physiological recordings in acute slices can only be performed in young animals (Fluegge et al., 2012), we repeated the co-immunoprecipitation experiments with lysates of olfactory epithelium of juvenile mice (postnatal day 0–5). The results obtained were very similar to those obtained from adult animals (Fig. 1F,G). However, a weak signal for a CNGA2–MUPP1 interaction was detectable in the lysates from juvenile mice (Fig. 1F).

Blocking of the interaction between MUPP1 and Olfr73

To investigate the physiological role of MUPP1, we designed an experimental strategy for disruption of MUPP1–olfactory-receptor interaction by loading olfactory neurons with a C-terminal peptide of an olfactory receptor. A peptide, comprising the last nine amino acids of the mGluR7a (a splice variant of Grm7) C-terminus (including the PDZ-ligand motif LVI), has previously been shown to block the binding of PICK1 and impair mGluR7a-dependent signaling in mouse cerebellar neurons (Bertaso et al., 2008). Based on this concept, and on our results showing that MUPP1 interacts with Olfr73 (Fig. 1), we produced a dominant-negative Olfr73 C-terminal peptide to uncouple the native receptor from the bound PDZ domain, thereby conferring an inhibitory function. Because our previous data has shown that the olfactory-receptor–PDZ interaction depends on the olfactory receptor C-terminus (Dooley et al., 2009), the synthetic inhibitory peptide was composed of the last 15 amino acids of the Olfr73 C-terminus (KDTVKKIIGTKVYSS).

To investigate whether the peptides did bind to MUPP1 as predicted, we analyzed the binding of MUPP1 to the Olfr73 C-terminal peptide. In one approach, we immobilized peptides onto a cellulose layer and performed interaction studies by incubating the microarrays with 2 µg of purified single PDZ domains (1 to 13) of MUPP1, which had additional HA-tags for detection. Bound PDZ domains were detected by incubation with antibody and chemiluminescence; purified GST was used as negative control. Peptide interaction assays were performed three times with each PDZ domain and interactions were scored positive when the signal was detected in all experiments. This analysis revealed that the Olfr73 C-terminus interacts with PDZ domains 2, 3, 4, 5, 7, 9, 10 and 13 of MUPP1 (Fig. 2A). This analysis was controlled by showing the binding of MUPP1 PDZ domains to the mGluR7 C-terminus (positive control), but not to the C-terminus of NMDAR2 (also known as GRIN2A) or the β2 adrenergic receptor (negative controls) (Cui et al., 2007). We also analyzed whether replacing the last and second-to-last amino acids of the Olfr73 C-terminus, both crucial in many PDZ-ligand interactions (Hung and Sheng, 2002), impaired the binding to PDZ domains. Because alanine substitutions are often used to abolish PDZ domain binding we tested the mutation (KDTVKKIIGTKVASA), but found that the binding appeared normal (Fig. 2A). The fact that tryptophan residues are rarely observed at the last and second-to-last amino acid positions in protein ligands of PDZ domains (Stiffler et al., 2007) led us to hypothesize that binding might be impaired in an Olfr73 tryptophan mutant (KDTVKKIIGTKVWSW). When tested, as predicted, this peptide did not interact with any PDZ domain in our assay (Fig. 2A). Moreover, binding of PDZ domains to other olfactory receptors (MOR16-1, MOR27-1, MOR36-1, MOR105-1, MOR109-1, MOR116-1, MOR129-2) was also abolished by introducing tryptophan at positions 0 and −2 (data not shown).

Co-immunoprecipitation of MUPP1 and Olfr73 from olfactory epithelium lysates was clearly abolished by adding 60 µM of inhibitory peptide (Olfr73 C-terminus KDTVKKIIGTKVYSS) to the reaction, whereas addition of 60 µM of the control peptide (Olfr73 tryptophan mutant KDTVKKIIGTKVWSW) resulted only in a weak inhibition of the interaction (Fig. 2B). Furthermore, we confirmed the interaction by analyzing the binding of the inhibitory peptide to one of the Olfr73-interacting PDZ domains of MUPP1. Because PDZ domain 13 could be expressed in relatively large amounts in bacteria, we chose this domain for the analysis. We coupled the peptide to the fluorophore Rhodamine B, incubated the labeled peptide and the purified PDZ domain and measured absorption at 543 nm to determine the amount of fluorescence that had bound to the PDZ domain (Fig. 2C). When comparing the binding of the inhibitory peptide and the control peptide, we found that ~60% more fluorescence was bound after incubation with the inhibitory peptide compared with that upon incubation with the control peptide (Fig. 2C). We then investigated whether binding of MUPP1 to other putative interaction partners also depends on the presence of the inhibitory peptide (Fig. 2D). The experiments revealed that precipitation of MUPP1 with ACIII did depend on the inhibitory peptide, whereas the interaction with CNGA4 was dependent on the inhibitory peptide to only a minor extent. These findings indicate that CNGA4 probably binds to PDZ domains that do not interact strongly with the receptor C-terminus, whereas ACIII, possibly, binds to domains that also interact with the receptor C-terminus (domain 8 and/or 13). Moreover, these results show that the presence of the inhibitory peptide disrupts the formation of the olfactory signaling complex that we demonstrated in Fig. 1.

Additionally, we undertook surface plasmon resonance analysis in order to quantify the interaction between PDZ domain 13 and the inhibitory peptide. After covalent

Journal of Cell Science (2014) 127, 2518–2527 doi:10.1242/jcs.144220

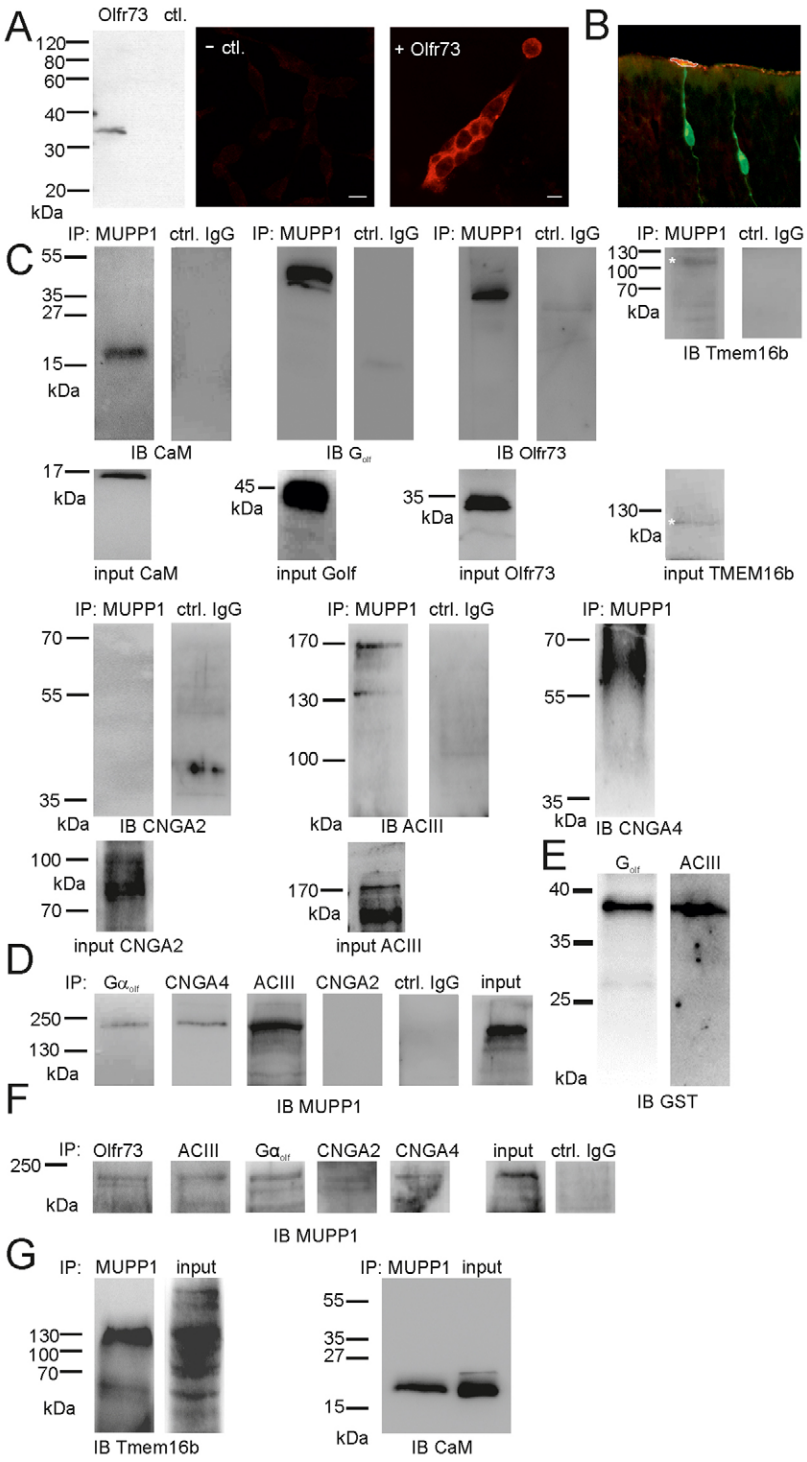

Fig. 1. MUPP1 interacts with various signaling proteins in olfactory sensory neurons. (A) Olfr73-transfected (+Olfr73) and non-transfected (− ctrl) HEK293 cells were stained with an antibody against Olfr73 (images on the right). Scale bar: 10 μm; Western blot analysis of Olfr73-transfected cells showing a specific band at 35 kDa, whereas no bands were detected in untransfected HEK293 cell lysates. (B) Staining of a cryosection of olfactory epithelium from a transgenic mouse expressing GFP (green) in all sensory neurons. Olfr73 expression was detected using an antibody against Olfr73 (red) and shows the labeling of cilia emanating from GFP-expressing cells, but not of cilia in non-labeled control cells. (C) Co-immunoprecipitation (from lysates of epithelium taken from mice less than 20 days post natum) of endogenous MUPP1 with calmodulin (CaM), $G\alpha_{olf}$, Olfr73, Tmem16b, CNGA2, ACIII and CNGA4. Murine olfactory epithelium lysate was immunoprecipitated (IP) with MUPP1 antibody or IgG as a control (ctrl) and detected with antibodies against the interacting protein (IB). (D) Co-immunoprecipitation (from lysates of epithelium taken from mice less than 20 days post natum) of endogenous $G\alpha_{olf}$, CNGA4, ACIII and CNGA2 with MUPP1. Murine olfactory epithelium lysate was immunoprecipitated with antibodies against the signaling proteins noted above or IgG as a control and then analyzed by western blotting with an antibody against MUPP1. (E) Interaction of $G\alpha_{olf}$ and ACIII with PDZ domain 13 of MUPP1 *in vitro*. $G\alpha_{olf}$ and ACIII were expressed in HEK293 cells, bound to beads and incubated with a PDZ-domain-13–GST fusion protein purified from bacteria. Binding of PDZ domain 13 was detected with an antibody against GST. (F) Co-immunoprecipitation (from lysates of epithelium taken from mice 0–5 days post natum) of endogenous Olfr73, ACIII, $G\alpha_{olf}$, CNGA2 and CNGA4 with MUPP1. Protein complexes were precipitated with antibodies against the proteins noted above or IgG and then analyzed by western blotting with an antibody against MUPP1. Olfactory epithelium lysate was loaded as an input control. (G) Co-immunoprecipitation (from lysates of epithelium taken from mice 0–5 days post natum) of endogenous MUPP1 with Tmem16b and calmodulin. Olfactory epithelium lysate was immunoprecipitated with MUPP1 antibody and western blotted with antibodies against the interacting protein. Input controls, 10% of the olfactory epithelium lysate that was used as starting material in the immunoprecipitations.

immobilization of the GST–PDZ13 fusion protein onto a CM5 chip surface (Biacore), the peptide was added at various concentrations, leading to increased responses (Fig. 2E). Fitting the exponential phase of the curves (first arrow in Fig. 2E) yielded the observed rate constants (k_{obs}) (Fig. 2F). The linear slope corresponds to the association rate constant (k_{on}) of the PDZ–peptide complex (0.036 $mM^{-1}s^{-1}$), the exponential fits to the dissociation phase (second arrow in Fig. 2F) and corresponds to the dissociation rate constant of the complex (k_{off}=0.013 s^{-1}), resulting in an equilibrium dissociation constant, K_d (k_{off}/k_{on} ratio), of 0.36 mM. The control peptide used in the same surface plasmon resonance experiment showed only background effects, which are common at high concentrations of analyte, and no exponential binding and no exponential decay kinetics (data not shown), proving that the binding affinity between the PDZ domain and inhibitory peptide is relatively weak but very specific.

Taken together, these experiments revealed that a C-terminal peptide of Olfr73 can bind to MUPP1 and that replacement of the residues at the last and second-to-last amino acid positions with

Journal of Cell Science (2014) 127, 2518–2527 doi:10.1242/jcs.144220

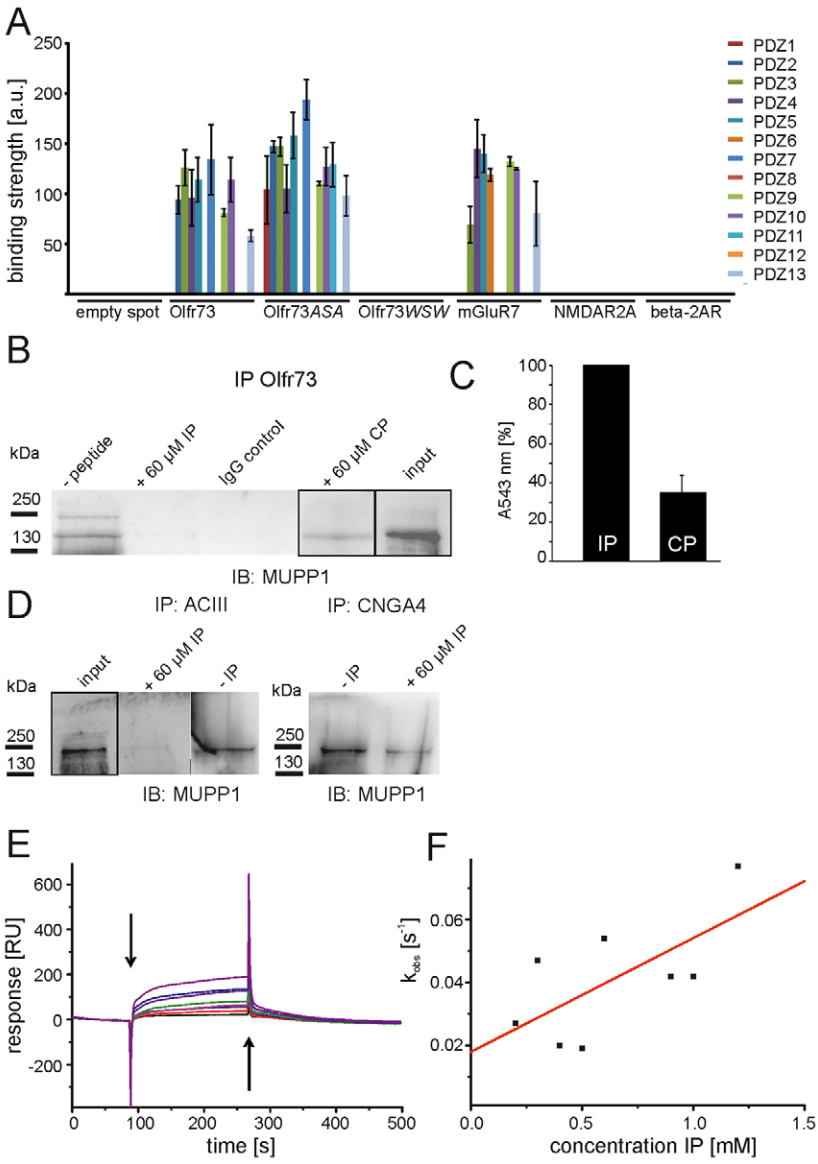

Fig. 2. Uncoupling of MUPP1 and Olfr73 using an inhibitory peptide. (A) Peptide-microarray-based Olfr73–PDZ interactions. The mean pixel densities resulting from incubation of individual PDZ domains of MUPP1 (1–13) with the spotted C-termini of Olfr73, Olfr73 with alanine mutations (Olfr73ASA), Olfr73 with tryptophan mutations (Olfr73WSW), mGluR7, NMDAR2A and β2AR are shown. Mean pixel densities were determined in triplicate, error bars are shown as s.e.m.; a.u., arbitrary units. (B) Co-immunoprecipitation of Olfr73 with MUPP1 from olfactory neurons without inhibitory peptide, 60 µM inhibitory peptide (IP) or 60 µM control peptide (CP). The middle lane shows an IgG control. The complex was precipitated with an antibody against Olfr73 and western blotted with an antibody against MUPP1 (IB). Olfactory epithelium lysate is shown as an input control. (C) Absorption at 543 nm to measure the binding of the Olfr73-interacting PDZ domain 13 (~15 µg) to the inhibitory or control peptides (2 mM) that had been coupled to Rhodamine B. The experiment was repeated three times. Absorption was measured in a photometer. Error bars are shown as s.e.m., n=3. (D) Co-immunoprecipitation of CNGA4 and ACIII with MUPP1 from olfactory neurons without inhibitory peptide (−IP) or 60 µM inhibitory peptide (+IP). Complexes were pulled down by using antibodies against ACIII and CNGA4 and detected with an antibody against MUPP1. (E) Typical surface plasmon resonance recordings of binding of the inhibitory peptide to GST–PDZ-domain-13, which had been immobilized on a CM5 chip. Starting at 0.2 mM the peptide concentrations were increased up to 1.2 mM (0.2 mM, 0.3 mM, 0.4 mM, 0.5 mM, 0.6 mM, 0.9 mM, 1.0 mM, 1.2 mM from the lowest to highest). As indicated by the arrows, the injection of peptide solution was started after 90 seconds (first arrow) and stopped after 270 seconds (second arrow). RU, relative units. (F) The observed rate constants, obtained from the fits to the exponential increase in panel C, are plotted against the inhibitory peptide concentration. The linear regression yields a slope value of 0.036 mM^{-1} s^{-1} and an intercept of 0.018 s^{-1}.

tryptophan residues abolishes binding. Importantly, the peptide can disrupt receptor–PDZ-domain binding when presented in excess to both binding partners and, thereby, act as inhibitor of the interaction between MUPP1 and Olfr73, whereas the mutated peptide does not.

Introduction of peptides into living sensory neurons

To introduce the Olfr73 peptides into living sensory neurons, we used acute slices of main olfactory epithelium from a transgenic mouse strain in which Olfr73-expressing neurons are labeled by eGFP (Oka et al., 2006). We introduced the inhibitory peptide and the control peptide into sensory neurons through a patch pipette (Fig. 3A). Because this approach has not been described before, we tested for peptide transport to the apical region of olfactory sensory neurons after insertion of the peptide at the cell soma by monitoring Rhodamine B fluorescence distribution in patch-clamped Olfr73 neurons by using confocal microscopy. Only green Olfr73-positive neurons that were attached to the recording pipette were loaded with the Rhodamine-B-coupled peptide, whereas adjacent green neurons, which were not patched, do not show red fluorescence (Fig. 3B). After insertion, Rhodamine B fluorescence was detected in the ciliary region by using microscopy (green cell labeled with a red fluorescent peptide in Fig. 3C). The translocation to the ciliary region was analyzed by eye, the mean translocation time was 139±16 s.

Uncoupling of the PDZ-olfactory-receptor interaction affects the odorant response

To analyze the electrophysiological properties of olfactory sensory neurons under control conditions, and during impaired binding to PDZ proteins, we introduced the inhibitory peptide and the control peptide into sensory neurons through a patch pipette. We recorded odor-evoked receptor currents in the whole-cell voltage-clamp configuration using the Olfr73 agonist vanillin (Oka et al., 2006). Because peptide diffusion to the ciliary compartment takes about 2 min, we measured olfactory sensory neuron responses to repeated vanillin applications over a time period of 5 min. The pipette solution contained no peptide, 6 or 60 µM inhibitory peptide or 60 µM control peptide. We stimulated olfactory sensory neurons by focal superfusion with

Journal of Cell Science (2014) 127, 2518–2527 doi:10.1242/jcs.144220

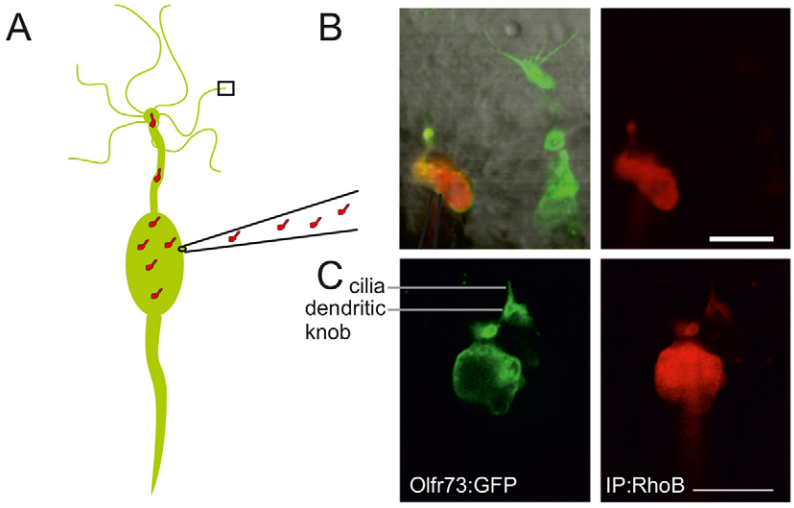

Fig. 3. Introducing Olfr73 inhibitory peptide into living sensory neurons. (A) After attaching an Olfr73 neuron to the recording pipette, the inhibitory peptide is transported to the site of signal transduction (black box). By binding to PDZ domains, the olfactory PDZ complex is disrupted. (B) Images, obtained by using confocal microscopy, of whole-cell patch clamping of olfactory neurons at −60 mV in acute slices of epithelium taken from GFP–Olfr73-expressing mice (green). The patch pipette was filled with intracellular solution mixed with 60 µM of inhibitory peptide that had been coupled to Rhodamine B. The left image shows a high-magnification overlay image of a patched neuron filled with inhibitory peptide (the far left neuron) and Olfr73-positive neurons (neurons on the right of the image, green). The right-hand panel shows an isolated image of the neuron that had been tagged with Rhodamine B fluorescence. (C) The Rhodamine-B-fused inhibitory peptide (IP; red in the image on the right) localized in the soma, dendrite, dendritic knob and cilia of the patched GFP-marked olfactory neuron (green in the image on the left) after an average of 2:19 min, (n=3). Scale bars: 5 µm.

100 µM vanillin (1 s; 60 s inter-stimulus interval) (Fig. 4A). For each cell, current amplitudes were normalized to the first response. Under control conditions (no peptide), odor-evoked currents declined over time (56% after 5 min, n=9) (Fig. 4A,B). In inhibitory-peptide-loaded neurons, we observed a significantly stronger peak current reduction after 5 min (91%, n=9) (Fig. 4A,B). When olfactory neurons were loaded with the control peptide, however, the decrease in current amplitude over time (45%, n=8) was similar to that of the control cells (Fig. 4A,B), Furthermore, the effects of the inhibitory peptide were dose-dependent, as 6 µM of the inhibitory peptide led to a current reduction of 77% after 5 min (n=8). These data show that PDZ-dependent organization is required for efficient activation of the intracellular signaling cascade.

In addition, we analyzed the kinetics of vanillin responses. The slope of the signal decreased in all tested conditions with repeated stimulus application. However, we could not detect any significant differences in neither the rise (Fig. 4C) nor the decay times (data not shown) between control cells and those treated with the inhibitory or control peptide after applying vanillin for 1 s.

Interruption of PDZ–olfactory-receptor binding affects the decline of the olfactory sensory neuron response

During sustained odorant exposure, olfactory sensory neuron receptor currents decline, despite the continued presence of the stimulus (Firestein et al., 1990; Reisert and Matthews, 1999; Zufall et al., 1991). We, therefore, asked whether MUPP1 affects sensory adaptation and analyzed current decay kinetics and peak–plateau ratios during prolonged stimulation with vanillin (5 s; 100 µM; one application after 3 min of incubation post insertion). Under these conditions, the decline of the receptor current followed a bi-exponential kinetic (Fig. 5A). Control neurons (unloaded and control-peptide-loaded cells) and inhibitory-peptide-loaded neurons showed marked differences in their adaptation kinetics. Inhibition of PDZ-domain binding changed the average plateau–peak ratio (Fig. 5B), the adaptation kinetics (Fig. 5C) and the inactivation time constant (Fig. 5D). The plateau–peak ratio of control cells and control-peptide-loaded cells was significantly lower than in inhibitory-peptide-loaded cells (Fig. 5B). The slow phase of the adaptation kinetic, represented by single exponential-fitted Tau values between 6 and 8 s of the recording (Fig. 5C), also differed significantly between control neurons (τ=0.6±0.05 s, n=7 for unloaded cells; τ=0.8±0.16 s, n=7 for control-peptide-loaded cells) and inhibitory-peptide-loaded neurons (τ=1.8±0.34 s, n=8), indicating a slowed response adaptation. Furthermore, we calculated the response termination kinetics as Tau values of a single exponential fit between 10 and 15 s of the recording (Fig. 5D). Again, there was a significant difference between the controls (τ=2.3±0.19 s, n=9 for unloaded cells; τ=2.2±0.1 s, n=9 for control-peptide-loaded cells) and inhibitory-peptide-treated neurons (τ=0.5±0.09 s, n=10), pointing to a faster termination of the response after prolonged odor stimulation, when the cell has already adapted. In summary, we conclude that PDZ-mediated organization of the signaling cascade is essential for proper termination of the odor response in olfactory neurons.

DISCUSSION

Response profiles and ligand sensitivity of olfactory receptors have been studied in the past, but other properties that might contribute to the odorant-induced responses – such as cytosolic interaction partners – have not been investigated. In this work, we studied the contribution of PDZ scaffolding proteins to the organization of transduction complexes coupled to olfactory receptors in the olfactory system. In order to analyze the physiological function of protein–protein interactions *in situ*, we developed an assay to disrupt the interaction in living sensory neurons. The approach involved the loading of a peptide encompassing the interaction domain of one binding partner through a patch pipette, leading to acute disruption of the complex in living cells. This might also be an advantageous technique for other cells that cannot easily be transfected or sustained in culture.

In most cases, PDZ domains assemble intracellular complexes by recognition of C-terminal sequences in their ligands. We have previously reported that MUPP1, a protein comprising 13 PDZ domains, can interact with olfactory receptors through their C-termini. Here, we performed a comprehensive interaction study with all 13 PDZ domains of MUPP1 and the C-terminus of murine Olfr73 using a peptide microarray and found that the peptide bound to most of the domains. Many PDZ domains have been grouped into three main specificity classes based on the last four amino acids of their ligands – class I domains bind to ligands with the sequence (-X-S/T-X-Φ), class II domains to (-X-Φ-X-Φ) and class III domains to (-X-X-C), where X is any residue and Φ

Journal of Cell Science (2014) 127, 2518–2527 doi:10.1242/jcs.144220

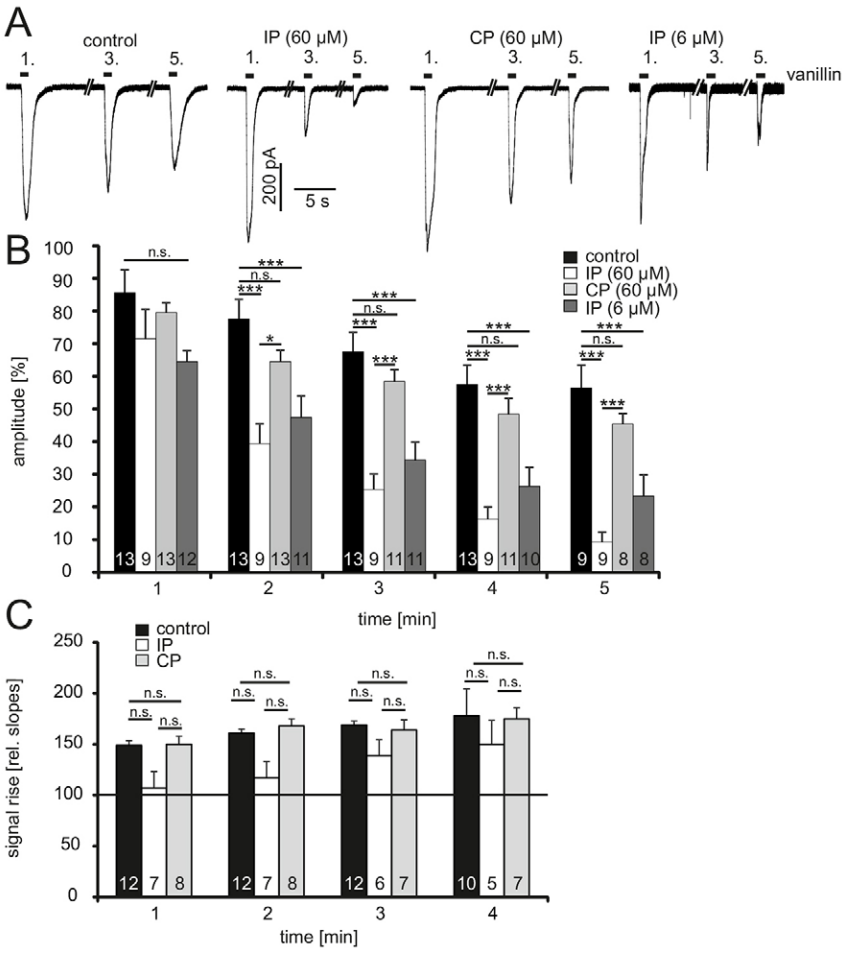

Fig. 4. Effects of PDZ–olfactory-receptor uncoupling on olfactory sensory neuron odor responses. (A) Representative traces of whole-cell patch clamp recordings from olfactory sensory neurons in acute slices of Olfr73 mice. Responses to the 1st, 3rd and 5th stimulus are shown. 100 µM vanillin was applied for 1 s every minute (indicated by the black bar). The holding potential was −60 mV. For PDZ–olfactory-receptor uncoupling, 6 µM or 60 µM of inhibitory peptide (IP) was added to the intracellular solution, 60 µM of control peptide (CP) that had been added to the intracellular solution served as control. (B) Normalized maximal amplitudes recorded from control cells, cells that had been infused with the inhibitory peptide and the control peptide in a time-dependent manner. The number in the column gives the number of measurements. Because all cells did not survive to record for 5 min, the number of cells measured decreases at higher times points. Peak receptor currents were normalized to the first current amplitude. (C) The normalized signal rise (relative slopes) of odor-induced current amplitudes for control cells and those treated with the inhibitory or control peptide. Error bars show the s.e.m. Significance levels were calculated using an ANOVA and Bonferroni multiple comparisons test: $*P<0.05$, $**P<0.01$, $***P<0.005$. ns, non-significant.

is a hydrophobic residue. This strict division of PDZ domains into three distinct classes has been questioned (Stiffler et al., 2007), and interactions exist which do not comply with these rules. Moreover, in some studies, it has been shown that not only the extreme C-terminus residues are important for binding but also that up to the last ten amino acids in a given protein might influence the binding energy. The Olfr73 C-terminus (-V-Y-S-S) has a class-II-like PDZ binding motif, although the last amino acid is not hydrophobic. The differences in PDZ domain binding that we observed when comparing the alanine substitutions at the 0 and −2 positions with the unchanged C-terminus could be explained by the fact that the C-terminus with alanine residues

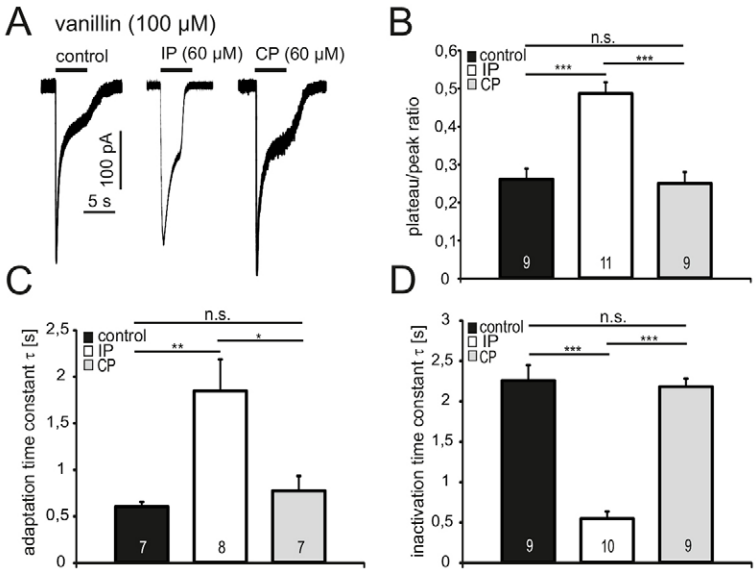

Fig. 5. Effects of PDZ-olfactory receptor uncoupling on response adaptation and termination. (A–C) Example traces of whole-cell patch clamp recordings of olfactory sensory neurons in acute slices of Olfr73 mice. At 3 min after insertion, 100 µM vanillin was applied once for 5 s (black bar). The holding potential was −60 mV. (A) Recording from a control cell. For PDZ–olfactory-receptor uncoupling, 60 µM of inhibitory peptide (IP) was added to the intracellular solution. As a control measurement, 60 µM of control peptide (CP) was added to the intracellular solution. (B) Plateau–peak ratios of control cells and cells that had been infused with the inhibitory peptide or the control peptide. A plateau was defined as the most horizontal area of the amplitude at the time of odor switch-off. (C) Tau values of adaptation kinetics of control cells and cells that had been treated with inhibitory peptide or control peptide after single exponential fitting of the curves between 6 and 8 seconds of the recordings. (D) Tau values of the termination kinetics of control cells and cells that had been treated with inhibitory peptide or control peptide, after single exponential fitting of the curves between 10 and 15 seconds of the recordings. Numbers in the columns indicate the number of measurements. Error bars show s.e.m. Significance levels were calculated using an ANOVA and Bonferroni multiple comparisons test. $*P<0.05$, $**P<0.01$, $***P<0.005$. ns, not significant.

Journal of Cell Science (2014) 127, 2518–2527 doi:10.1242/jcs.144220

still resembles a class II PDZ ligand. Although not markedly different from the wild-type peptide, the peptide with the alanine substitutions bound additional PDZ domains. Possibly, the larger tyrosine residue in the wild-type peptide prevents binding of the peptide to PDZ domains, which prefer smaller hydrophilic residues at this position. The peptide with tryptophan mutations did not bind MUPP1 PDZ domains.

We found that MUPP1, similarly to *Drosophila* InaD in the visual system, coordinates the recruitment of components that are involved in both activation ($G\alpha_{olf}$, ACIII and CNGA4, Tmem16b) and deactivation (calmodulin). Taken together, our results suggest that the assembly of signaling molecules into organized transducisome complexes is an important aspect of odorant detection. PDZ proteins have been shown to increase the speed and the efficiency of G-Protein-coupled receptor (GPCR) signaling by acting as scaffolds, thereby tethering downstream effectors in close proximity to the receptor. A strong indication for the existence of an olfactory PDZ complex is that, apart from co-localization of MUPP1 and diverse signaling proteins in cilia and dendritic knobs (Dooley et al., 2009), our co-immunoprecipitation experiments demonstrated an interaction between MUPP1 and $G\alpha_{olf}$, ACIII, CNGA4, Tmem16b, calmodulin and Olfr73 in juvenile and adult mice. MUPP1 has previously been shown to regulate the coupling of G proteins to the melatonin receptor (MT_1) (Guillaume et al., 2008), and other PDZ proteins, such as NHERF-1 and NHERF-2 (also known as SLC9A3R1 and SLC9A3R2, respectively), can modulate interactions between GPCRs and heterotrimeric G proteins (Rochdi et al., 2002; Wang et al., 2010). The G protein γ 13 subunit (Gγ13), which is abundantly expressed in the cilia of olfactory sensory neurons (Kerr et al., 2008), has been shown to bind MUPP1 in taste bud cells (Liu et al., 2012).

The physiological functions of MUPP1 were studied *in situ* after disruption of the interaction between an olfactory receptor and MUPP1 in mouse olfactory neurons. For this, the C-terminus of Olfr73 was introduced into neurons that endogenously expressed Olfr73, and vanillin-induced receptor currents were recorded. Recordings of the odorant-induced receptor currents revealed that interruption of the olfactory-receptor–PDZ interaction resulted in a strong reduction of current amplitudes, indicating the essential role of PDZ-protein-based scaffolding in olfactory signal transduction. The reduction in current amplitude is in accordance with our interaction partner analysis, as impaired clustering of the receptor with $G\alpha_{olf}$, ACIII, CNG channel proteins and Tmem16b could explain such a decrease in the olfactory signaling efficiency. If olfactory-receptor–$G\alpha_{olf}$ coupling is diminished in peptide-loaded neurons, olfactory signaling is expected to be strongly impaired (Belluscio et al., 1998). Enhanced signal transduction of GPCRs has been described for several PDZ proteins, including InaD, which tethers downstream effectors in close proximity to rhodopsin in *Drosophila* visual signal transduction (Scott and Zuker, 1998), thereby dramatically increasing the amplitude and speed of the physiological response to light. In mammalian cells, proteins such as NHERF have been found to enhance the efficiency of GPCR-stimulated G protein signaling (Ardura and Friedman, 2011).

Here, we report decelerated response adaptation and faster response termination during, and after, prolonged (5 s) odorant stimulation when the receptor–PDZ interaction is inhibited. A similar effect of interrupted PDZ modulation has also been demonstrated in a previous study, in which a faster decay time of $GABA_B$ receptor signaling was found after knockdown of MUPP1 (Balasubramanian et al., 2007). In contrast with this effect, we did not detect any significant differences in signal termination after short odor stimulation (1 s). However, signal termination mechanisms could be dependent on the length of the application of the odor – stimulated olfactory neurons can reach adaptation during stimulus application.

A reduction in the amount of MUPP1 resulted in prolonged Ca^{2+} responses, evoked by the activation of an odorant receptor in the recombinant expression system (Dooley et al., 2009). This discrepancy, compared with the sensory neurons, most likely results from a different set of MUPP1 binding partners in the recombinant expression system (HEK293 cells), where not all proteins of the olfactory signaling cascade are present. The dynamics of the odorant-induced responses in the recombinant expression system indicated an interaction of olfactory receptors with MUPP1 but did not help to elucidate the function of MUPP1 in sensory neurons (Dooley et al., 2009), which has been addressed in the present study.

The observed acceleration of odor response termination could be caused by the lack of complex formation with ACIII, possibly resulting in faster termination of the cAMP supply close to the CNG channel after stimulus withdrawal. Mislocalization of the Ca^{2+}-binding factor calmodulin, which together with Ca^{2+} renders the CNG channel less sensitive to cAMP (Song et al., 2008), could lead to slowed adaptation of the response during sustained odorant exposure. Calmodulin has also been shown to modulate channel properties by activating calmodulin kinases through direct interaction with the *Drosophila melanogaster* PDZ protein InaD (Chevesich et al., 1997; Xu et al., 1998), and MUPP1 has been shown to bind to the calmodulin-dependent kinase CaMKII (Ackermann et al., 2009). However, as patch clamp experiments on acute slices are limited to early postnatal (day 0–5) mice (smooth cranium), potential differences in the function of MUPP1 in adult mice cannot be excluded. Even if the MUPP1-organized olfactosome is present in both newborn and adult mice, we cannot rule out a different physiological importance, as olfactory sensory neurons undergo functional changes from postnatal day 0 through to day 30 (Belluscio et al., 1998; Lee et al., 011).

Taken together, these results show that the scaffolding protein MUPP1 is essential for the organization of complex and dynamic olfactory signaling, influencing not only signal generation but also response termination and adaptation.

MATERIALS AND METHODS

Antibodies

The primary antibodies used were against: MUPP1 (a rabbit polyclonal provided by Hermann Luebbert, Ruhr-Universität Bochum, Germany; and mouse monoclonal, catalog number 1510), $G\alpha_{olf}$ (rabbit polyclonal, catalog number 1209; goat polyclonal, catalog number 26764), HA (mouse monoclonal, catalog number H9658, Sigma-Aldrich), TMEM16b (rabbit polyclonal, Rasche et al., 2010), calmodulin (mouse monoclonal, catalog number 137079), CNGA2 (goat polyclonal, catalog number 13700), CNGA4 (goat polyclonal, catalog number 167508), adenylyl cyclase III (goat polyclonal, catalog number 32113; rabbit polyclonal, catalog number 588), GST (rabbit polyclonal, catalog number 459). Unless stated otherwise, antibodies were purchased from Santa Cruz Biotechnology. Normal rabbit IgG was also used (catalog number 2729, Cell Signaling Technology). For generation of an antibody against Olfr73, the Basic Local Alignment Search Tool (BLAST) was used to identify a unique sequence motif. The antibody was raised against a peptide from the C-terminus (CKDTVKKIIGTKVYSS) by Eurogentec Deutschland GmbH (Köln, Germany). The specificity of the antibody was shown by immunohistochemical staining and western blot analysis of Olfr73-transfected HEK293 cells (Fig. 1A). The secondary antibodies used were horseradish peroxidase (HRP)-coupled goat anti-mouse,

donkey anti-goat and goat anti-rabbit IgGs (1:10,000) (Bio-Rad, München, Germany), and goat anti-rabbit or -mouse IgG conjugated to Alexa Fluor 546 or 660 (Molecular Probes).

Co-immunoprecipitation and western blotting

Co-immunoprecipitation was performed with olfactory epithelium lysate from BL6 mice (postnatal day 5–20), which was minced in RIPA buffer [150 mM NaCl, 50 mM Tris-HCl, 1% Nonidet, 0.5% sodium deoxycholate (w/v), 0.1% SDS (w/v) and protease inhibitors] using the Catch & Release system (Catch & Release v2.0, Millipore). Samples were centrifuged at 1000 ***g*** for 10 min followed by another preparation with RIPA buffer and centrifugation. Afterwards, both supernatants were pooled. The lysate (4 mg total protein) was incubated with primary antibodies (each 0.8 µg) overnight at 4℃ in a spin column. After several washing steps, the proteins were eluted from the column using a denaturing elution buffer. Unspecific IgG (0.8 µg) was used for precipitation as control (n=2 or 3). In total, 25 female and 28 male adult mice, and 62 female and 57 male juvenile mice were used for the co-immunoprecipitation experiments.

To specifically interrupt the MUPP1–Olfr73 interaction, 60 µM of an inhibitory peptide (the last 15 C-terminal amino acids of Olfr73) or 60 µM of a control peptide (tryptophan mutant) was added to the olfactory epithelium lysate samples and co-immunoprecipitation was performed as described above. Protein samples were loaded on an SDS gel and subjected to immunoblotting (Porablot NCL nitrocellulose membrane, Machery-Nagel). Interactions were detected by using specific antibodies (1:50–1:250) and the enhanced chemiluminescence (ECL) detection system (n=3, from a total of 14 female and 13 male mice).

Peptide *in vitro* interaction study

For *in vitro* interaction studies, HEK293 cells were transfected with the respective pcDNA3 constructs (15 µg; ACIII, G_{olf}). Specific antibodies against ACIII and G_{olf} were biotinylated using the EZ-Link Micro Sulfo-NHS-Biotinylation Kit (Thermo Scientific). HEK293 protein lysates were incubated for 2 hours at 4℃ with 2 µg of the respective antibodies, and the antibody bound proteins were purified using the Dynabeads FlowComp Flexi kit (Invitrogen). After several washing steps, Dynabeads were incubated with the recombinant PDZ domain GST fusion proteins (~15 µg) overnight at 4℃. The samples were subjected to SDS gel electrophoresis and immunoblotting, interactions were detected by using an antibody against GST (1:250) and the ECL detection system.

DNA constructs

GST fusion constructs of the PDZ domains 1–13 of MUPP1 were generated by cloning the single domains into the pGEX-3X expression vector (Amersham Pharmacia Biotech), pCDNA3-MUPP1 served as template. Primer sequences are given in supplementary material Table S1. All constructs were verified by sequencing.

Peptide microarrays

Single PDZ domains of MUPP1 (1–13) were produced in *E. coli* BL21 DE3pLysS. The culture was induced using 0.5–1 mM Isopropyl β-D-thiogalactoside (IPTG) and purified by using glutathione-coupled Sepharose beads (Becton Dickinson Biosciences). Accurate protein sizes were verified by electrophoresis and Coomassie staining, protein concentrations were measured using a Bradford assay (Coomassie Plus Protein Assay, Thermo Scientific).

CelluSpots™ Peptide Arrays (Intavis AG) were blocked for 2 hours at room temperature with 3% of a protein mixture (3K Eiweiss Shake, Layenberger) in NaCl, Tris, Tween-20 and incubated with the single PDZ domains (2 µg protein) of MUPP1 fused to HA, followed by detection with an antibody against HA (1:250) and HRP-coupled secondary antibodies using the ECL Plus western blotting detection reagent (GE Healthcare). Binding was considered positive when a signal was detectable in all three experiments. The microarray data were obtained using Vilber Lourmat Fusion Software. Data concerning the binding affinity were analyzed with TIGR Spotfinder 3.2.1. The intensities (0–255) were calculated as mean values for spots where a positive signal was observed in all three experiments. Results are presented as mean±s.e.m.

Peptide synthesis

Enantiomerically pure fluorenylmethyloxycarbonyl chloride (Fmoc) amino acids were purchased from Iris Biotech (Marktredwitz, Germany) or Novabiochem (Laufelfingen, Switzerland). Ser(tBu)-Wang (0.8 mmol/g) and Trp(OtBu)-Wang (0.48 mmol/g) resins were from Novabiochem, the coupling reagents 1-hydroxybenzotriazole (HOBt), 2-(1H-benzotriazole-1-yl)-1,1,3,3-tetramethyluronium tetrafluoroborate (TBTU) and N,N-diisopropylethylamine (DIPEA) were from Iris Biotech. Peptide-grade dimethylformamide (DMF) was obtained from Roth (Karlsruhe) and Rhodamine B (99+ %) from Acros (Geel, Belgium).

The peptide sequences were synthesized on an automated microwave peptide synthesizer (Liberty-CEM) according to the manufacturer's instructions at a scale of 0.1 mmol using the Fmoc strategy. The amino acids (four equivalents) were coupled stepwise with HOBt (four equivalents), TBTU (four equivalents) and DIPEA (six equivalents) at 75℃, 30 W, 300 seconds in DMF. Fmoc deprotection was accomplished by treatment with 20% piperidine in DMF (cycle 1: 75℃, 35 W, 30 seconds; cycle 2: 75℃, 50 W, 180 seconds). Semi-preparative purification was performed on a Knauer smartline high-performance liquid chromatography (HPLC) with a 4-wavelength detector and a Varian Dynamax Microsorb C-18 reversed-phase column (250×10 mm) with a gradient of 5–80% acetonitrile in 25 min. Analytical runs were performed on the same instrument using a Varian Dynamax Microsorb 100-5 C-18 reversed-phase column (250×4.6 mm) with a gradient of 10–85% acetonitrile in 30 min. Mixtures of Millipore^R water and acetonitrile with 0.1% trifluoroacetic acid (v/v) were used as eluents at a flow rate of 4–5 ml/minute and 0.75 ml/minute, respectively. All chromatograms were recorded at λ=215 and/or 254 nm. LC-MS analyses were carried out on an Agilent 1100 instrument coupled to a Bruker Esquire 6000 mass spectrometer. An Agilent Zorbax SB-C18 column was used (2.1×50 mm, 1.8 µm) with Millipore^R water (supplemented with 0.05% TFA) and acetonitrile (Baker, HPLC grade) as eluents. Routinely, the gradient was 0–100% acetonitrile in 10 min with a flow rate of 0.3 ml/minute with detection at λ=220 or 254 nm. Electrospray ionization mass spectrometry spectra were measured on a Bruker Esquire 6000 mass spectrometer. The mass to charge relation (m/z) is given as a dimensionless number. The Fmoc-deprotected Ser(tBu)-Wang resins were cleaved, precipitated and subjected to purification by semi-preparative HPLC (KDTVKKIIGTKVYSS 80 mg (0.064 mmol), yield 38 mg of crude product; KDTVKKIIGTKVWSW 193 mg (0.093 mmol), yield 84 mg of crude product).

Coupling of Rhodamine B (three to four equivalents) to the deprotected N-terminus was performed manually in a plastic syringe (5 ml, BD Pharmingen) with a porous disc as filter, using HOBt (three to four equivalents), TBTU (three to four equivalents) and DIPEA (ten equivalents). The mixture was shaken at room temperature for 4 hours in the dark followed by excessive washing with DMF, dichloromethane (DCM) and methanol. The resin was dried *in vacuo*. The crude products were cleaved from the resin by treatment with TFA:TIS:water (95:2.5:2.5) for 3 hours at room temperature, followed by precipitation in ice-cold diethyl ether and isolation by centrifugation. Following purification by HPLC, the product fractions were pooled and lyophilized. Inhibitory peptide: 35 mg (0.028 mmol) resin-coupled peptide, 40 mg (0.084 mmol, 3 eq) of Rhodamine B, 13 mg (0.084 mmol, three equivalents) HOBt, 27 mg (0.084 mmol, three equivalents) TBTU and 46 µl (0.28 mmol, 10 eq) DIPEA. Control peptide: 105 mg (0.048 mmol) resin-coupled peptide, 92 mg (0.192 mmol, four equivalents) of Rhodamine B, 29.4 mg (0.192 mmol, four equivalents) HOBt, 61.7 mg (0.192 mmol, four equivalents) TBTU and 79.3 µl (0.48 mmol, ten equivalents) DIPEA.

Peptide interaction assays

Recombinant PDZ domain 13 (~15 µg) was solubilized in interaction buffer (10 nM HEPES, 100 mM KCl, 0.5 mM EDTA, 1 mM DTT and protease inhibitors, pH 6.5), and unspecific interactions were blocked

using the interaction buffer with additional 1% bovine serum albumin. 2 mM of inhibitory peptide or control peptide were added to PDZ domain 13 and incubated for 3 hours at 4°C. After several washing steps with the interaction buffer, the absorption was measured in a photometer at 543 nm (n=3). The mean values of the control peptide measurement were normalized to the inhibitory peptide mean values.

To specifically interrupt the MUPP1–Olfr73 interaction, 60 µM of an inhibitory peptide (the last 15 C-terminal amino acids of Olfr73) was added to the olfactory epithelium lysate samples and co-immunoprecipitation was prepared as described above. Protein samples were loaded on a SDS gel and subjected to immunoblotting (Porablot NCL nitrocellulose membrane, Machery-Nagel). Interactions were detected by using specific antibodies (1:50–1:250) and the ECL detection system (n=3).

Surface plasmon resonance

The interaction between PDZ domain 13 and the inhibitory and control peptides was analyzed by surface plasmon resonance using the Biacore 3000 system (GE Healthcare). Recombinant GST–PDZ-domain-13 (10 µM) was immobilized on a CM5 chip by EDC-NHS chemical crosslinking according to the manufacturer's protocol. A pH scouting assay indicated an optimum pH value of 5.0 for the immobilization procedure (10 mM acetic acid buffer). The control lane was treated in the same manner but used GST protein for immobilization. A flow rate of 10 µl/minute was employed throughout all experimental steps. After immobilization, the surfaces were washed with NaCl (1 mol/L) and SDS (0.05%) for 1 minute each. For the following experiments, a buffer was used that contained 10 mM HEPES, 143 mM NaCl, 0.05% P20 surfactant, pH 7.1. In separate experiments the inhibitory peptide and the control peptide were run at various concentrations (each from 0.1 mM up to 2 mM) over the PDZ domain and the control lane. The association, as well as the dissociation, phase was recorded for 3 min, afterwards the surfaces were rinsed with NaCl and SDS (concentrations as above) for complete regeneration of the immobilized protein. For data analysis, the recordings of the control lane were subtracted from those of the PDZ lane. Three independent sets of experiments were carried out comprising all steps described, including the immobilization of freshly prepared GST–PDZ-domain-13. Reproducible and consistent recordings of peptide binding were obtained.

Olfactory epithelium preparation

Transgenic mice expressing Olfr73–GFP (postnatal day 0–5, a total of 64 female and 40 male mice) (Oka et al., 2006) were sacrificed using CO_2 followed by decapitation. The mouse head was dissected in ice-cold oxygenated extracellular solution and embedded in 4% (w/v) low-gelling-temperature agarose (Sigma-Aldrich, Munich, Germany). Acute coronal olfactory epithelium slices (300-µm) were cut with a vibratome (VT1000S, Leica Microsystems, Wetzlar, Germany) and collected in a Perspex chamber filled with cooled oxygenated extracellular solution until measurement. The extracellular solution contained 120 mM NaCl, 25 mM $NaHCO_3$, 5 mM KCl, 1 mM $CaCl_2$, 1 mM $MgSO_4$, 1 mM *N,N*-Bis-(2-hydroxyethyl)-2-aminoethane sulfonic acid (300 mOsm, pH 7.3).

Electrophysiology

Acute olfactory epithelium slices were electrophysiologically characterized by using a recording chamber (Slice Mini Chamber, Luigs and Neumann) and a confocal microscope (Leica DM 6000 CFS, Leica Microsystems) to visualize single neurons. A steel wired slice-hold-down (SHD26H/15, Hugo Sachs Elektronik, Harvard Apparatus GmbH) was used to fix the acute slices, which were submerged with oxygenated extracellular solution. Patch pipettes (6–9 MΩ) were pulled from borosilicate glass capillaries (GB150TF-8P, Science Products) using a PC-10 vertical two-step puller (Narishige Instruments) and fire-polished using a MF-830 Microforge (Narishige Instruments). Experiments were performed under optical control in the whole-cell configuration and recorded using an EPC-10 amplifier controlled by PatchMaster 2.20 (HEKA Elektronik, Lambrecht/Pfalz, Germany). The recording pipette solution contained 143 mM KCl, 10 mM HEPES, 1 mM EGTA, 2 mM KOH, 1 mM MgATP, 0.5 mM NaGTP (290 mOsm, pH 7.1). The calculated liquid junction potential (JP-CalcW software) was automatically subtracted online. The pipette and cell membrane capacitance were also automatically compensated during the measurement. The experiments were performed by applying continuously oxygenated extracellular solution and using a holding potential of −60 mV. The recordings were filtered using Bessel filters at 10 kHz and at 2.9 kHz. The signals were sampled at 10 kHz. Odorants were applied using a pressure-driven microcapillary application system. Slices were used for just one measurement to exclude odorant contamination of yet untreated cells.

Data analysis

Electrophysiological data were analyzed off-line using IGOR Pro 6.05 (Wave Metrics) with Neuromatic 2.0 (Jason Rothman) and Excel 2010 (Microsoft) software. To calculate the signal rise, single traces were mono-exponentially fitted. The response decay was calculated as decay time constants (τ). Here, single traces were mono-exponentially fitted during distinct time periods (6–8 seconds for adaptation kinetics and 10–15 seconds for response termination kinetics).

The microarray data were obtained using VilberLourmat Fusion Software. Spot intensities were analyzed with TIGR Spotfinder 3.2.1. Intensities (0–255) were calculated as mean values for spots where a positive signal was observed in all of the repeat experiments. The individual highest intensity of one array was set as 100% and all other intensity values were normalized to this. Statistical analysis was performed by applying repeated measurement ANOVA, Bonferroni multiple comparison tests and the Mann–Whitney U test using Statistica (StatSoft) or unpaired Student's t-test as a built in function in Excel. P values were assessed as follows: 0.05<*; 0.01<**; 0.005<***. Results are presented as mean±s.e.m.

Acknowledgements

We thank K. Touhara (The University of Tokyo, Tokyo, Japan) for the donation of Olfr73 transgenic mice, and H. Luebbert (Ruhr-University Bochum, Bochum, Germany) for the donation of MUPP1 antibodies. B. Hoffknecht (Ruhr-University Bochum, Bochum, Germany) is acknowledged for help with the peptide synthesis.

Competing interests

The authors declare no competing interests.

Author contributions

E.M.N., M.S. and H.H. were responsible for the original concept of the research. Research was designed by E.M.M., M.S., C.H., N.M.N. Data were collected by S.B., F.J., W.B., B.K., F.K., S.D.K., P.S., S.R., R.D., and analyzed by S.B., C.H., M.S., E.M.N. The manuscript was written by E.M.N., S.B. and M.S.

Funding

This work was supported by the Deutsche Forschungsgemeinschaft [grant numbers SFB958, SFB642 and Exc257], the Studienstiftung des deutschen Volkes, the International Max-Planck Research School in Chemical Biology (IMPRS-CB), the Ruhr-University Research School and the Wilhelm und Guenter Esser-Stiftung. M.S. is a Lichtenberg-Professor of the Volkswagen Foundation.

Supplementary material

Supplementary material available online at
http://jcs.biologists.org/lookup/suppl/doi:10.1242/jcs.144220/-/DC1

References

Ackermann, F., Zitranski, N., Borth, H., Buech, T., Gudermann, T. and Boekhoff, I. (2009). CaMKIIalpha interacts with multi-PDZ domain protein MUPP1 in spermatozoa and prevents spontaneous acrosomal exocytosis. *J. Cell Sci.* **122**, 4547-4557.

Ardura, J. A. and Friedman, P. A. (2011). Regulation of G protein-coupled receptor function by Na+/H+ exchange regulatory factors. *Pharmacol. Rev.* **63**, 882-900.

Bakalyar, H. A. and Reed, R. R. (1990). Identification of a specialized adenylyl cyclase that may mediate odorant detection. *Science* **250**, 1403-1406.

Balasubramanian, S., Fam, S. R. and Hall, R. A. (2007). GABAB receptor association with the PDZ scaffold Mupp1 alters receptor stability and function. *J. Biol. Chem.* **282**, 4162-4171.

Belluscio, L., Gold, G. H., Nemes, A. and Axel, R. (1998). Mice deficient in G(olf) are anosmic. *Neuron* **20**, 69-81.

Bertaso, F., Zhang, C., Scheschonka, A., de Bock, F., Fontanaud, P., Marin, P., Huganir, R. L., Betz, H., Bockaert, J., Fagni, L. et al. (2008). PICK1 uncoupling from mGluR7a causes absence-like seizures. *Nat. Neurosci.* **11**, 940-948.

Bhandawat, V., Reisert, J. and Yau, K. W. (2005). Elementary response of olfactory receptor neurons to odorants. *Science* **308**, 1931-1934.

Bhandawat, V., Reisert, J. and Yau, K. W. (2010). Signaling by olfactory receptor neurons near threshold. *Proc. Natl. Acad. Sci. USA* **107**, 18682-18687.

Billig, G. M., Pál, B., Fidzinski, P. and Jentsch, T. J. (2011). Ca2+-activated Cl− currents are dispensable for olfaction. *Nat. Neurosci.* **14**, 763-769.

Bockaert, J., Fagni, L., Dumuis, A. and Marin, P. (2004). GPCR interacting proteins (GIP). *Pharmacol. Ther.* **103**, 203-221.

Castillo, K., Restrepo, D. and Bacigalupo, J. (2010). Cellular and molecular Ca2+ microdomains in olfactory cilia support low signaling amplification of odor transduction. *Eur. J. Neurosci.* **32**, 932-938.

Chevesich, J., Kreuz, A. J. and Montell, C. (1997). Requirement for the PDZ domain protein, INAD, for localization of the TRP store-operated channel to a signaling complex. *Neuron* **18**, 95-105.

Cui, H., Hayashi, A., Sun, H. S., Belmares, M. P., Cobey, C., Phan, T., Schweizer, J., Salter, M. W., Wang, Y. T., Tasker, R. A. et al. (2007). PDZ protein interactions underlying NMDA receptor-mediated excitotoxicity and neuroprotection by PSD-95 inhibitors. *J. Neurosci.* **27**, 9901-9915.

Cygnar, K. D. and Zhao, H. (2009). Phosphodiesterase 1C is dispensable for rapid response termination of olfactory sensory neurons. *Nat. Neurosci.* **12**, 454-462.

Dhallan, R. S., Yau, K. W., Schrader, K. A. and Reed, R. R. (1990). Primary structure and functional expression of a cyclic nucleotide-activated channel from olfactory neurons. *Nature* **347**, 184-187.

Dooley, R., Baumgart, S., Rasche, S., Hatt, H. and Neuhaus, E. M. (2009). Olfactory receptor signaling is regulated by the post-synaptic density 95, Drosophila discs large, zona-occludens 1 (PDZ) scaffold multi-PDZ domain protein 1. *FEBS J.* **276**, 7279-7290.

Firestein, S., Shepherd, G. M. and Werblin, F. S. (1990). Time course of the membrane current underlying sensory transduction in salamander olfactory receptor neurones. *J. Physiol.* **430**, 135-158.

Fluegge, D., Moeller, L. M., Cichy, A., Gorin, M., Weth, A., Veitinger, S., Cainarca, S., Lohmer, S., Corazza, S., Neuhaus, E. M. et al. (2012). Mitochondrial Ca(2+) mobilization is a key element in olfactory signaling. *Nat. Neurosci.* **15**, 754-762.

Guillaume, J. L., Daulat, A. M., Maurice, P., Levoye, A., Migaud, M., Brydon, L., Malpaux, B., Borg-Capra, C. and Jockers, R. (2008). The PDZ protein mupp1 promotes Gi coupling and signaling of the Mt1 melatonin receptor. *J. Biol. Chem.* **283**, 16762-16771.

Hengl, T., Kaneko, H., Dauner, K., Vocke, K., Frings, S. and Möhrlen, F. (2010). Molecular components of signal amplification in olfactory sensory cilia. *Proc. Natl. Acad. Sci. USA* **107**, 6052-6057.

Hung, A. Y. and Sheng, M. (2002). PDZ domains: structural modules for protein complex assembly. *J. Biol. Chem.* **277**, 5699-5702.

Kerr, D. S., Von Dannecker, L. E., Davalos, M., Michaloski, J. S. and Malnic, B. (2008). Ric-8B interacts with G alpha olf and G gamma 13 and co-localizes with G alpha olf, G beta 1 and G gamma 13 in the cilia of olfactory sensory neurons. *Mol. Cell. Neurosci.* **38**, 341-348.

Kleene, S. J. (2008). The electrochemical basis of odor transduction in vertebrate olfactory cilia. *Chem. Senses* **33**, 839-859.

Kobayakawa, K., Hayashi, R., Morita, K., Miyamichi, K., Oka, Y., Tsuboi, A. and Sakano, H. (2002). Stomatin-related olfactory protein, SRO, specifically expressed in the murine olfactory sensory neurons. *J. Neurosci.* **22**, 5931-5937.

Lee, A. C., He, J. and Ma, M. (2011). Olfactory marker protein is critical for functional maturation of olfactory sensory neurons and development of mother preference. *J. Neurosci.* **31**, 2974-2982.

Liu, Z., Fenech, C., Cadiou, H., Grall, S., Tili, E., Laugerette, F., Wiencis, A., Grosmaitre, X. and Montmayeur, J. P. (2012). Identification of new binding partners of the chemosensory signaling protein Gγ13 expressed in taste and olfactory sensory cells. *Front Cell Neurosci.* **6**, 26.

Nickell, W. T., Kleene, N. K. and Kleene, S. J. (2007). Mechanisms of neuronal chloride accumulation in intact mouse olfactory epithelium. *J. Physiol.* **583**, 1005-1020.

Oka, Y., Katada, S., Omura, M., Suwa, M., Yoshihara, Y. and Touhara, K. (2006). Odorant receptor map in the mouse olfactory bulb: in vivo sensitivity and specificity of receptor-defined glomeruli. *Neuron* **52**, 857-869.

Rasche, S., Toetter, B., Adler, J., Tschapek, A., Doerner, J. F., Kurtenbach, S., Hatt, H., Meyer, H., Warscheid, B. and Neuhaus, E. M. (2010). Tmem16b is specifically expressed in the cilia of olfactory sensory neurons. *Chem. Senses* **35**, 239-245.

Reisert, J. and Matthews, H. R. (1999). Adaptation of the odour-induced response in frog olfactory receptor cells. *J. Physiol.* **519**, 801-813.

Reisert, J., Lai, J., Yau, K. W. and Bradley, J. (2005). Mechanism of the excitatory Cl- response in mouse olfactory receptor neurons. *Neuron* **45**, 553-561.

Rochdi, M. D., Watier, V., La Madeleine, C., Nakata, H., Kozasa, T. and Parent, J. L. (2002). Regulation of GTP-binding protein alpha q (Galpha q) signaling by the ezrin-radixin-moesin-binding phosphoprotein-50 (EBP50). *J. Biol. Chem.* **277**, 40751-40759.

Schreiber, S., Fleischer, J., Breer, H. and Boekhoff, I. (2000). A possible role for caveolin as a signaling organizer in olfactory sensory membranes. *J. Biol. Chem.* **275**, 24115-24123.

Scott, K. and Zuker, C. S. (1998). Assembly of the Drosophila phototransduction cascade into a signalling complex shapes elementary responses. *Nature* **395**, 805-808.

Song, Y., Cygnar, K. D., Sagdullaev, B., Valley, M., Hirsh, S., Stephan, A., Reisert, J. and Zhao, H. (2008). Olfactory CNG channel desensitization by Ca2+/CaM via the B1b subunit affects response termination but not sensitivity to recurring stimulation. *Neuron* **58**, 374-386.

Stephan, A. B., Shum, E. Y., Hirsh, S., Cygnar, K. D., Reisert, J. and Zhao, H. (2009). ANO2 is the cilial calcium-activated chloride channel that may mediate olfactory amplification. *Proc. Natl. Acad. Sci. USA* **106**, 11776-11781.

Stiffler, M. A., Chen, J. R., Grantcharova, V. P., Lei, Y., Fuchs, D., Allen, J. E., Zaslavskaia, L. A. and MacBeath, G. (2007). PDZ domain binding selectivity is optimized across the mouse proteome. *Science* **317**, 364-369.

Ullmer, C., Schmuck, K., Figge, A. and Lübbert, H. (1998). Cloning and characterization of MUPP1, a novel PDZ domain protein. *FEBS Lett.* **424**, 63-68.

Wang, B., Ardura, J. A., Romero, G., Yang, Y., Hall, R. A. and Friedman, P. A. (2010). Na/H exchanger regulatory factors control parathyroid hormone receptor signaling by facilitating differential activation of G(alpha) protein subunits. *J. Biol. Chem.* **285**, 26976-26986.

Xu, X. Z., Choudhury, A., Li, X. and Montell, C. (1998). Coordination of an array of signaling proteins through homo- and heteromeric interactions between PDZ domains and target proteins. *J. Cell Biol.* **142**, 545-555.

Zheng, J. and Zagotta, W. N. (2004). Stoichiometry and assembly of olfactory cyclic nucleotide-gated channels. *Neuron* **42**, 411-421.

Zufall, F. and Leinders-Zufall, T. (2000). The cellular and molecular basis of odor adaptation. *Chem. Senses* **25**, 473-481.

Zufall, F., Shepherd, G. M. and Firestein, S. (1991). Inhibition of the olfactory cyclic nucleotide gated ion channel by intracellular calcium. *Proc. R. Soc. B* **246**, 225-230.